PCCP

ROYAL SOCIETY OF CHEMISTRY

PAPER

View Article Online
View Journal

Check for updates

Cite this: DOI: 10.1039/d3cp02912c

The boson peak in silicate glasses: insight from molecular dynamics†

Ahmed El Hamdaoui, *[a] El Mehdi Ghardi,*[b] Achraf Atila, [c]
Hicham Jabraoui, [de] Michael Badawi, [f] Abdellatif Hasnaoui [g] and
Said Ouaskit*[a]

Received 22nd June 2023,
Accepted 23rd October 2023

DOI: 10.1039/d3cp02912c

rsc.li/pccp

In the low-frequency regime, ≈1 THz, glasses show an anomalous excess in their vibrational density of states called the boson peak (BP). The origin of BP has been a subject of debate since its first discovery a few decades ago. Although BP has been the focus of numerous studies, no conclusive answers have been found about its origins, which remained elusive to date. Here, we present results based on molecular dynamics of several binary and ternary silicate glasses with different network intermediates and modifier oxides. The vibrational density of states and the BP are reported for all the studied glasses. Their correlation with the elastic constant C_{44}, structural, and dynamical properties are extensively discussed in terms of Voronoi atomic volume and the vibrational mean square displacement of Q_4 species specifically. We also question the classical classification of alkali oxides as modifiers, and we suggest that Li_2O plays the role of pseudo-intermediate oxide in lithium silicate glasses. This claim is supported by the effect of Li on various vibrational modes, and this effect differs from the other alkali metals. Furthermore, we demonstrate a correlation between the BP intensities and both the Voronoi volume of the Q_4 and Q_3 units and vibrational mean square displacements.

1. Introduction

The vibrational density of states (VDOS) in glasses exhibits an excess of vibrational modes around frequencies near 1 THz, deviating from the ω^2 Debye's law. This excess emerges in the specific heat of glasses at low temperatures, around 10 K, which is larger than that of crystals that follow Debye's known T^3 law. This vibrational anomaly is referred to as the boson peak (BP).[1–3] It is a universal behavior appearing in disordered media, and it is affected in glasses by the structural properties, the medium-range order, and the dynamics of the super-cooled liquids. This anomaly of glassy states has been demonstrated for years in infrared absorption,[4,5] low-frequency Raman,[6,7] and in inelastic neutron scattering spectra[8–10] for a very large set of glasses.

Even though the origin of the BP is still under debate, several attempts were suggested to explain its relationship with the glassy state. For example, the phonon saddle transition model explains the appearance of the BP based on a sharp phase transition between the phonon-free phase and amorphous elastic phase one.[11] Another attempt was suggested by the soft potential model, in which vibrations in the BP region were considered to come from both localized tunneling and soft vibrational states.[12–14] In a further approach, the elastic heterogeneity theory predicts the BP as a manifestation of the inhomogeneity in the mechanical response of glasses at the nanoscale.[15–18] On the other hand, in the quasi-localized mode model, the BP is explained by the existence of low-frequency, non-propagating vibrational modes centered around defects in the glass structure. The interaction between the quasi-localized modes with the surrounding elastic media results in a spread of their frequencies and intensities, which causes the BP.[19,20] A large number of models and theories giving different explanations of this anomaly demonstrate how complex the nature of vibrations in the BP region is, which continues to be a long-standing mystery in condensed matter physics.

For silicate-based glasses, many attempts of correlation with physical parameters are proposed in the literature for the

---

[a] Laboratoire de Physique de la Matière Condensée, Faculté des Sciences Ben M'sik, University Hassan II of Casablanca, B.P. 7955, Av Driss El Harti, Sidi Othmane, Casablanca, Morocco. E-mail: elhamdaouiahmed96@gmail.com, s.ouaskit@gmail.com

[b] Nuclear Futures Institute, Bangor University, Gwynedd, LL57 2DG, UK. E-mail: m.ghardi@bangor.ac.uk

[c] Department of Material Science and Engineering, Saarland University, Saarbrücken, 66123, Germany

[d] Université Paris-Saclay, NIMBE, CEA, CNRS, F-91191 Gif-sur-Yvette Cedex, France

[e] LAAS-CNRS, University of Toulouse, 31077 Toulouse, France

[f] Université de Lorraine, F-54000, Nancy, France

[g] LS2ME, Faculté Polydisciplinaire Khouribga, Sultan Moulay Slimane University of Beni Mellal, B.P. 145, 25000 Khouribga, Morocco

† Electronic supplementary information (ESI) available. See DOI: https://doi.org/10.1039/d3cp02912c

origins of the BP. Starting from systematic studies of the effect of ionic radius,[21] field strength,[22] and mass[23] of the cations on the BP, studies were extended to cover also the effect of the degree of polymerization as demonstrated by Richet.[24] Besides the atomic properties and the role of oxides, other physical properties such as the effect of fictive temperature of the glass,[25] the fragility index of the predecessor liquid[26] and elastic properties[27] were also reported. On the other hand, the topological aspects of silicate glasses and their correlation with the BP are rarely considered. Attempts[28,29] to link its frequency with the FSDP (First Sharp Diffraction Peak) have been suggested. However, the very origin of the FSDP and what it represents in the structure of glass itself remains a subject of debate.

Here, in this work, we attempt to identify an appropriate correlation between the structure, composition, glass properties, and the BP anomaly in silicate glasses using molecular dynamics (MD) simulations. In our previous works,[30–32] the structure–property relationship has been studied as a function of composition. The structural change in silicate glasses has been discussed in detail according to different types of oxides, demonstrating their different roles in establishing their macroscopic properties.[30–32] To study the effect brought by different network intermediates and modifier oxides on structural and vibrational properties, two ternary glasses $BaO–TiO_2–SiO_2$ (BTS) and $CaO–Al_2O_3–SiO_2$ (CAS), and three binary silicate glasses $(M_2O)–(SiO_2)$ with M = Li, Na, and K were chosen in this investigation. The molar concentration of different types of oxides was varied to identify the relationship of Q_n species population which are by definition the network formers or intermediates surrounded by n bridging oxygens (oxygen atoms that are shared between two network formers and/or intermediates), their local Voronoi atomic volume (VAV), and dynamics with the BP.

2. Computational details

2.1. Glass preparation

The glasses of interest were simulated using MD simulations by adopting the rigid ionic model to represent atoms in our systems.[33–35] The details of compositions, simulation protocols, and the interactions are described in detail in the ESI† [36] and can be found in ref. 30–32. The structure factor for one composition of each system was calculated and presented in the ESI.† Concerning the coordination number, we define it by calculating the number of neighboring atoms within a certain specified distance from a central atom. During the simulation, we tracked the positions of atoms over time and calculated the distances between each atom and its neighboring atoms. An atom was considered a neighbor if its distance from the central atom fell within a predefined cutoff distance. The coordination number for a central atom was then determined by counting the number of neighbors that satisfied this distance criterion. Furthermore, the fractions of the Q_n units as a function of modifier concentrations are reported in Fig. 2 in the ESI† [36] for all studied binary systems (LS, NS and KS). For ternary systems the results have already been reported in Ghardi *et al.* and Atila *et al.*[30,31]

To underline the straightforward effect of modifiers and their content on the vibrational spectra of binary silicate glasses, the compositions of the binary alkali glasses lithium silicate (LS), sodium silicate (NS), and potassium silicate (KS) were varied from 5 to 30%. For the ternary systems, the content of the intermediate oxide was changed in a manner that will take into consideration the effect of the [intermediate]/[modifer] ratio and [intermediate]/[former] ratio for the CAS and the BTS systems respectively. These different ratios were considered to distinguish any dependence on composition that can alter the effect of intermediate oxides on the BP.[31] Some snapshots of the 25% composition of each studied glass are presented in Fig. 1. All MD simulations were performed using the LAMMPS package.[37]

2.2. VDOS calculation

To compute the vibrational density of states (VDOS), two methods can be used: (i) diagonalization of the dynamical matrix obtained from the finite displacement method or (ii) the Fourier transform of the velocity auto-correlation function (VACF).

$$g_{\mathrm{FFT}}(\omega) = \frac{1}{NK_{\mathrm{B}}T}\int\frac{\mathrm{d}t}{2\pi}\exp(iwt)\left\langle\sum_{i}^{N} v_i(0)v_i(t)\right\rangle \tag{1}$$

In this work, the latter method was adopted since it is more efficient when dealing with a large number of atoms.[38] To measure the VDOS, the VACF of all the structures was computed during MD runs. First, each system was equilibrated for 1 ns at a low temperature (50 K) in the canonical ensemble *NVT* with a timestep of 1 fs. Then, the VACF was computed using the microcanonical ensemble *NVE* for 200 ps with a timestep of 0.1 fs. In this case, the averaging is done every 20 timesteps for a total of 200 000 timesteps. The obtained VDOS for pure silica glass is shown and compared with experimental data in Fig. S1 (ESI†).[36]

2.3. Elastic properties

The stiffness matrix is the key for extracting elastic properties of materials, which can be calculated *via* energy minimization[39] at zero temperature with the obtained glass configurations from MD simulation as an input (20 configurations for each composition in all studied systems). This matrix can be obtained by taking the second derivative of the energy w.r.t. strain within the limit of small deformations:[40]

$$C_{ij} = \frac{1}{V}\left(\frac{\partial^2 U}{\partial\varepsilon_i\partial\varepsilon_j}\right), \tag{2}$$

where V is the volume. For isotropic materials, after calculating the stiffness matrix, the shear modulus was calculated as follows:

$$G = \frac{C_{44} + C_{55} + C_{66}}{3} \tag{3}$$

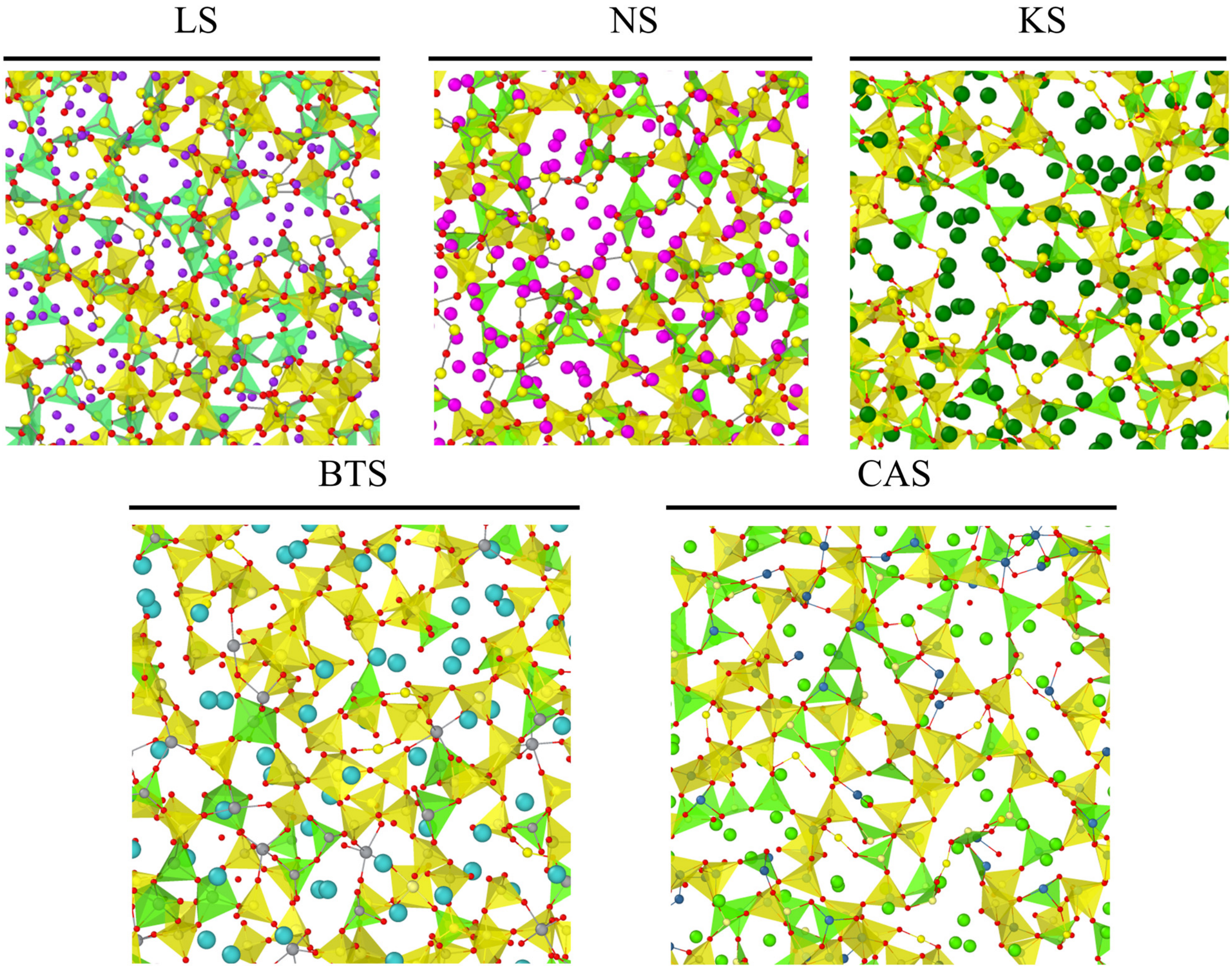

Fig. 1 Snapshots for 25% composition for all studied systems. The yellow polyhedra are the Q_4 units and the lime polyhedra are the Q_3 units of Si atoms in all systems and other intermediates Al and Ti for CAS and BTS respectively. The colors of the atoms are as follows (O = red, Si = yellow, Li = purple, Na = pink, K = green, Ca = lime, Ba = cyan, Ti = grey, Al = blue-gray).

3. Results and discussion

3.1. Vibrational density of states

Fig. 2(a) presents the VDOS of LS, NS, and KS glasses for the 25% composition altogether with the spectrum of pure silica as a reference (for other glasses with all compositions, see the ESI,† Fig. S2–S6[36]). The spectrum of pure silica shows two bands as generally accepted.[24,41] The upper band ($\omega \geq 20$ THz) represents the optic branch with two pronounced peaks connected to the transverse and longitudinal elongation of the SiO_4 tetrahedra. The structure of the lower band is more complicated because of the overlap between the optical and acoustic branches. A mode assignment[42,43] analysis for the SiO_4, Si–O–Si, and O–Si–O units in the upper band demonstrated that the dominant contribution of the two peaks corresponds to the asymmetric stretching of the Si–O–Si units and SiO_4 between 32 and 37 THz. For the lower band, the bending of the O–Si–O units and the rocking modes of the SiO_4 units are dominant in this region.[44–46] A predominant mode has also been identified in the region between 5 to 7 THz linked to the coupled rotations of SiO_4.[44] This special mode is described by the displacement of rigid units when the oxygen around a fixed Si atom is displaced. This coupled rotation of SiO_4 has been previously related to vibrations in the region of the BP by Buchenau *et al.*,[44] although this image has been corrected by Taraskin *et al.*[47] who demonstrated that the contribution of coupled rotations to the modes is not significant on this vibrational excess. A sketch representing those modes is presented in Fig. 3.

The comparison between the LS spectrum with that of pure silica shows a widening of the upper band and a narrowing of the lower band accompanied by a reduction of the gap between the two bands. This reduction is driven by the splitting of the upper band in which new modes appear in the frequency region 21.5–32 THz. This behavior, generally linked to the effect of the dominant species in the network, which is oxygen, can be interpreted in terms of the vibrational modes of the forming units of the network. As described previously, the dominant vibration modes in the lower band are the bending of O–Si–O bonds, the rocking modes of SiO_4 tetrahedra, and the

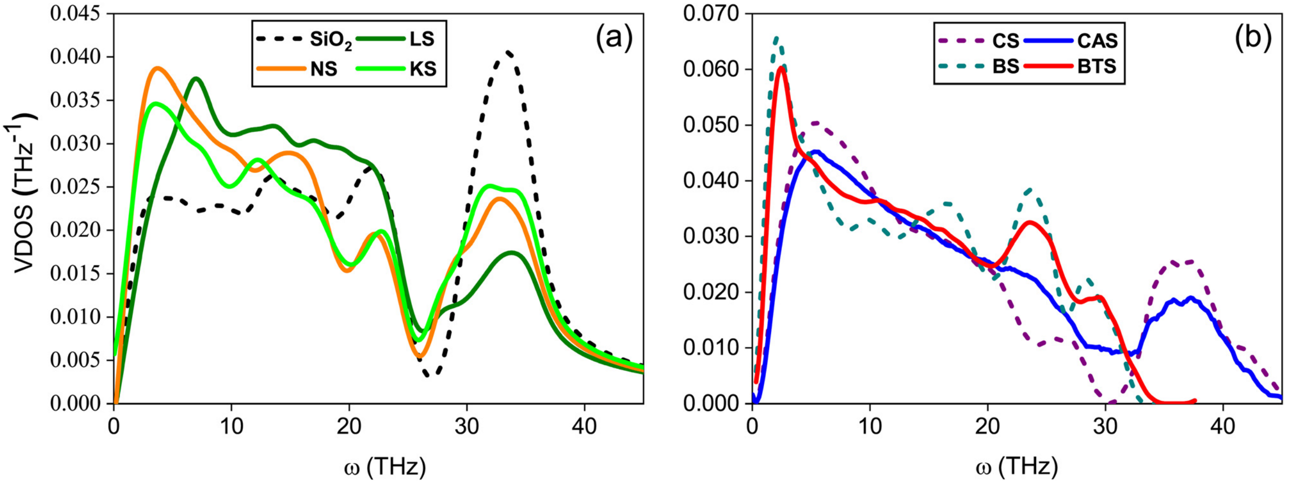

Fig. 2 Vibrational density of states plotted as a function of frequency. (a) For glasses with alkali oxide modifiers Li, Na, and K with pure silica as reference. (b) For the x = 25% composition of BTS and CAS systems with CS and BS as references.

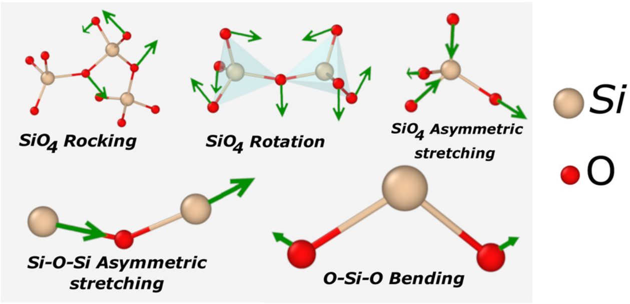

Fig. 3 Sketch of the vibrational modes in pure silica as an example case.

coupled and uncoupled rotational modes of SiO_4. The appearance of the non-bridging oxygens (NBOs) in the structure mainly leads to a reduction in the Si–O bond length so that asymmetric vibrations such as rocking modes are favored. It is also expected that the uncoupled rotation modes will become more dominant than the coupled rotation modes as Li_2O is added to the system.

Moving on to the NS and KS glasses, the shape of their vibrational spectrum does not vary much from pure silica. The effect of Na and K appears to be very different from that of Li_2O. Comparing the upper band to the lower band, the density of the vibrational modes decreases in both bands up to the low-frequency region between 1 and 10 THz approximately, where Na and K add new modes. This is in qualitative agreement with the observations reported previously.[41,48,49] According to the decomposition of the NS glass VDOS, made by Kilymis *et al.*,[50] the contribution of oxygen atoms is dominant across the spectrum, and that of Na and K atoms is typically below ≈11 THz.[49] Mode analysis of Si–O–Si units has shown that their vibrations up to ≈21 THz are rocking and bending modes, while above this frequency, they are stretching modes.[51,52] A small shift in the mean contribution of the Si–O–Si units modes is also observed in Fig. 2(a) towards ≈22.5 THz due to the widening of the angle between the atoms of these units. Concerning the upper high-frequency band, a significant overlap is seen between the contribution of NBOs and the contributions of species Q_2 and Q_3.

The effect of intermediate oxides on the vibrational spectrum is presented in Fig. 2(b) with 25% of TiO_2 and Al_2O_3 for BTS and CAS glasses, respectively. The effect of adding Al_2O_3 on the shape of the VDOS produced by our simulations is in agreement with the experimental data provided by inelastic neutron scattering[53] and *ab initio* simulation.[54] In Fig. 2(b), the VDOS shows two bands; the main band between 1 and 25 THz, and a high-frequency band between 30 and 45 THz. As shown, the main features of the VDOS of silicate glass are conserved for a wide range of compositions and oxides.[55] In particular, the VDOS of CAS glasses is almost similar to that of NS glasses. The infrared spectroscopic mode assignment study by Hwa *et al.*[56] demonstrated that the vibrational modes of the high-frequency peak are similar to those of amorphous silica. The decrease in the intensity of this band is mainly due to the decrease in the SiO_2 content in CAS glasses. Regarding the intermediate band, the supplementary modes akin to adding alumina are attributed to the bending of Al–O–Al and Al–O–Si bonds[56] and are accentuated depending on the composition. For the low-frequency region, and as seen in binary glasses, the dominant modes are attributed to the Ca^{2+} network modifier with its weaker binding to oxygen.[56,57]

For the BTS glass, the vibrational spectrum shows three bands. The upper band is attributed to Q_2 and Q_3 of the SiO_4 tetrahedra, and the 23 THz band is attributed to vibrational modes of silicon atoms with their oxygen environments.[58,59] The lower band in the 10 THz region has been interpreted to originate from the vibration of Ba–O.[60] This interpretation is based on the absence of this band in binary TiO_2–SiO_2 glasses.[61] Important similarities in the Raman spectrum between the crystalline phase and the glass phase have also been reported by several authors.[60,62,63] The BTS glasses considered in our simulations have a composition relatively close to the Fresnoite crystal, and therefore a mode assignment based on these previous studies is reliable. The Raman spectrum of fresnoite glass reveals an intense peak at 25 THz corresponding to the shortening of the Ti–O bond in TiO_5 groups.[64] In this configuration, apical (out-of-plane) oxygen is strongly bound to titanium, forming what can be thought of as a Ti=O double bond. The effect of the addition of TiO_2 should linearly increase the intensity of this peak in VDOS, which is not observed in Fig. 2(b). This is mainly due to the simplistic type of pair potential used to describe the Ti–O bond.

3.2. Structural correlation length

The frequency of the BP is related to a correlation length l_c that has been employed to calculate the medium-range order for glassy systems.[65,66] This length is measured as the ratio between the phonons transverse acoustic velocity and the BP frequency, according to the relationship:

$$l_c = \frac{V_T}{\omega_{BP}}, \quad V_T = \sqrt{\frac{G}{\rho}} \tag{4}$$

with V_T the transverse speed of sound and ω_{BP} the BP frequency. The frequency ω_{BP} was calculated from the normalized vibrational density of states $(g(\omega)/\omega^2)$ and the transverse velocity of sound was estimated from the calculated shear modulus and the glass density. The calculated BP frequencies for each system are reported in the ESI,† Table SII[36].

The value of this structural length represents the crossover from affine to nonaffine elasticity below which the system homogeneity is broken,[67] and it is found to be in the order of a few tens of atoms or nanometers.[67,68] As a result, the correlation length is expected to be smaller for a more dense structure compared to the open ones. This expectation was confirmed previously by Ando *et al.*[7] for binary SiO_2–Al_2O_3, aluminosilicate and other glassy systems studied by Schroeder *et al.*[69] and in other works including densified silicate glass.[70,71] Fig. 4, represents the dynamic correlation length of all studied glasses with varied concentrations of intermediates and modifiers alkali oxides. For the pure silica, the value of l_c from our simulations was found to be 3.5 nm, in good agreement with the findings of Carini Jr *et al.*[70] and Ando *et al.*[7] who reported values of 3.7 nm and 3.8 nm respectively. For binary glasses, Fig. 4, shows a fluctuating trend and gives no clear conclusion about the relationship of this property with the composition of binary glasses, while for ternary glasses, l_c appears to stay nearly constant. The comparison between these two classes of glassy systems with v-SiO_2 emphasizes that the high value of the correlation length observed in alkali-silicate systems compared to the BTS and CAS is a signature of the low elastic homogenization in the nanometric scale, which results from the addition of alkali oxide modifiers compared to the introduction of the intermediate oxides to the structure of silica.

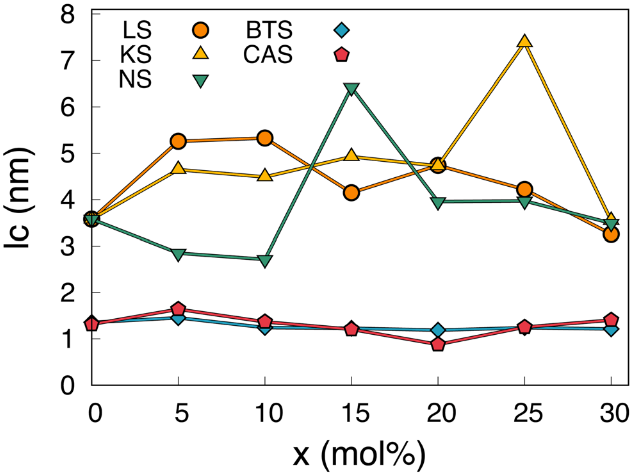

Fig. 4 Correlation length lc for all studied systems.

Apart from that, a comparison between the vibrational spectra in the VDOS of intermediates and alkali oxide modifiers, especially in the lower band as seen in Section 3.1, shows a clear tendency of the modifiers to add more vibrational modes in contrast to the intermediate oxides. Not only that but also the increase of the BP intensity (see the ESI,† Fig. S2–S4[36]) is an indication of the enhancement of the soft elastic modes,[71] which were shown in previous reports to introduce higher correlation length.[72] In addition, the dropping of the correlation length from 3.5 nm in v-SiO_2 to ≈1.3 nm and ≈1.3 nm in BTS and CAS, respectively, indicates the reduction of the poorly packed structural domains enclosed in the network of silicate glass. Be that as it may, this approach does not give a clear correlation with the effect of the concentration of the alkali oxide modifiers or intermediates.

3.3. Correlation with physical properties

To illustrate the effect of the different oxides studied in this paper, we have plotted as a function of the elastic constant C_{44} the different intensities of the BP obtained from each glass in Fig. 5. The observed correlation of the BP with the shear modulus is based on the study of Shintani *et al.*[73] where they demonstrated that the transverse character of vibrations is governing in the BP region. We found that, depending on the composition, the modifiers Na and K decrease the elasticity and increase its vibrational excess, while adding Ti/Al intermediates has the opposite effect. For LS glasses, although the Li cations depolymerize the network and promote the creation of NBOs, the glass rigidity increases and the intensity of the BP decreases, thus showing intermediate-like behavior, as shown in Fig. 5. Similar observations on the effect of Li and low coordination modifiers in the aluminosilicate glasses were reported previously.[74,75] A correlation with the ionic radius of the alkali oxide modifier cations can also be noticed (Fig. 5), which is considerable and consistent with Richet's findings.[21,24]

To understand the behavior observed in LS glasses, it is necessary to discuss the classification of the different oxides in forming a vitreous network. Among the first theories suggested for classifying glass oxides is Zachariasens random network theory.[76] The main rules to classify an oxide are the

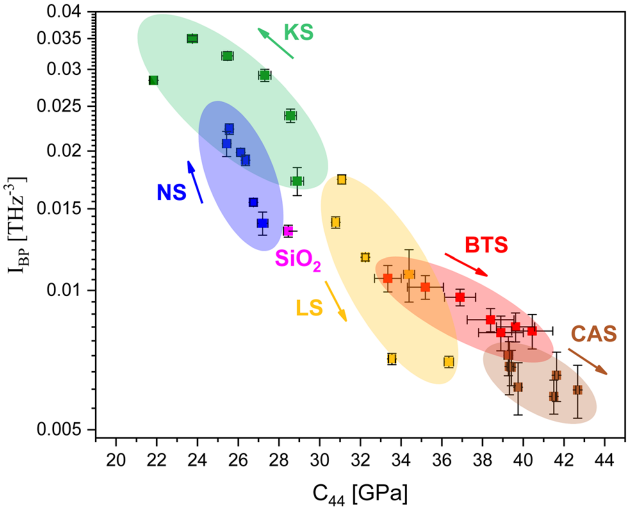

Fig. 5 The intensity of the BP of VDOS as a function of the elastic constant C_{44}. The arrows describe the direction of increasing modifier content increase in alkali silicate glasses and intermediate oxide in the BTS and CAS glasses.

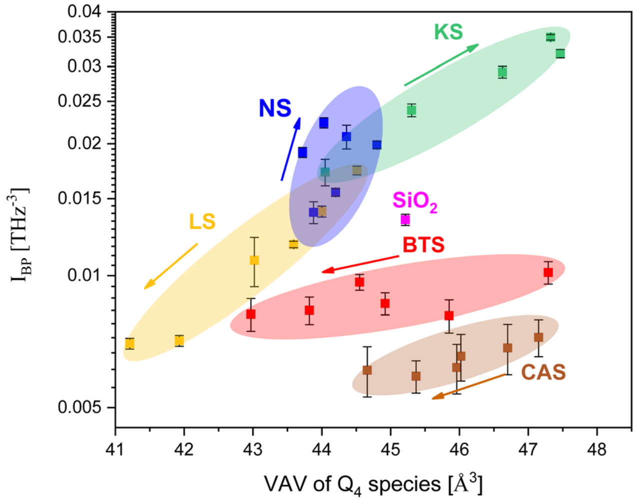

Fig. 6 The intensity of the BP as a function of Q_4 species Voronoi atomic volume. Arrows represent the ascending direction of intermediates and modifiers content. The error bars of the VAV are smaller than the symbols.

coordination number and polyhedral connectivity modes. Applying these rules to Li_2O, it will be considered as a modifier. The same goes for other theories using different parameters to classify oxides, such as Dietzel's[77] theory which relies on the notion of field strength, and Sun's[78] and Rawson's[79] theory based on the bond energy of M–O bonds.

The classical role attributed to Li^+ as a modifier is to depolymerize the network and decrease the rigidity of the glasses. Therefore, one should expect an increase in the intensity of the BP with increasing Li_2O content. However, if we see the results presented in this paper, the composition dependence correlation of the BP intensities and the other properties, *e.g.*, C_{44} is positive in the case of NS and KS glasses while it is negative in the case of LS glasses. This observation makes these classifications not fully descriptive and cannot be applied to all oxides. To explain the behavior of Li^+, we can start by looking at its local effect in the glasses. As it has a low average coordination number (≈ 3.6) compared to the other alkali cation (≈ 4.5 for Na and ≈ 8.3 for K), the presence of some regions that have even lower coordination numbers than the average makes Li cations strongly bonded to oxygen atoms giving rise to the increased local strength of the glass network. This anomaly that appears in the case of lithium has been observed in recent studies by Pedone,[39] who reported that lithium appears to behave like a network intermediate by forming a 4-fold coordinate, resulting in an increase in network cross-linking and cohesion in silicate glasses, which explains the rise in experimental elastic constant values in comparison to silica glass.[80] Furthermore, Pedone *et al.*[39] and Du *et al.*[81] reported another anomalous behavior of lithium on the characteristic correlation length compared to other alkali elements. They reported that the characteristic correlation length increases in the case of lithium silicate glasses while it decreases for other alkali silicate glasses. These results highlighted that lithium increases the intermediate range order due to its large field strength compared to the other alkali elements.

One expects that the mechanical properties of oxide glasses decrease with increasing modifier content; however, as we mentioned earlier and as shown in the literature, the increase of lithium in the glass causes an increase in the elasticity modulus.[85] Although the oxidation state is argued to remain the same, lithium ions adopt different coordination numbers depending on the global and local compositions. This change in the coordination number of lithium leads to a significant change in the field strength, which is reflected in the increase of the elastic moduli. This behavior has been observed for many cations that are classically seen as modifiers, but in practice, they behave like intermediate oxides in the glass network.[82] With this said, it is necessary to consider the modifiers network and distribution in the glass matrix to describe the glass properties properly.

Based on the structural analysis carried out previously on the atomic volume distribution of Voronoi,[32] Fig. 6 shows the intensity of the BP as a function of the average VAV of Q_4 units. All points seem to have a positive correlation with the VAVs of Q_4 units in agreement with the picture given by Nakamura *et al.* on the effect of atom volume.[27] The advantage of the correlation observed in Fig. 6 compared to that of C_{44} is that it also takes into account the size of the cations added to the different glasses. It should be noted that the volumes considered in ternary glasses also take into account the Q_4 formed by the Ti and Al atoms.

In order to further examine how the local structure affects the BP, we show in Fig. 7 the BP intensities as a function of the VAVs of Q_3 units for the binary silicate glasses. For the 3 systems, the BP intensities show a clear correlation with the Q_3 VAVs, with a positive correlation for LS glasses and a negative correlation for the NS and KS glasses. Furthermore, a correlation with the ionic radius of the alkali oxide modifiers

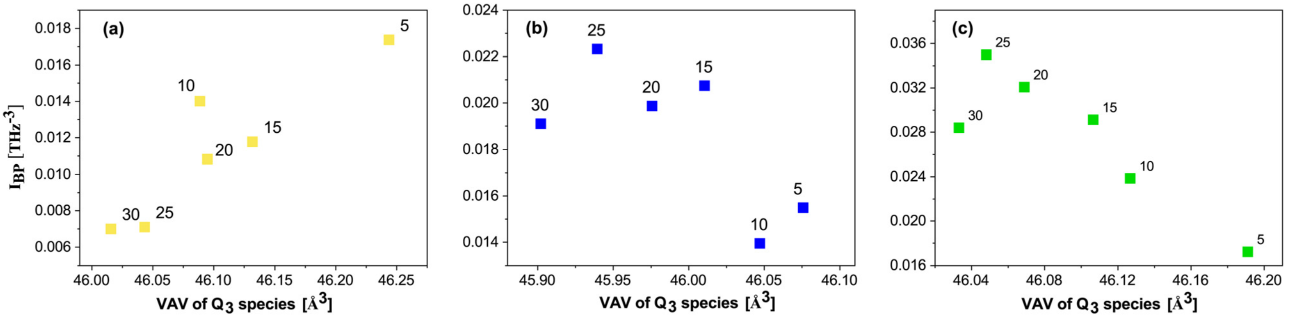

Fig. 7 The intensity of the boson peaks of VDOS as a function of the atomic volume of Voronoi of Q_3 species. (a) For LS glasses, (b) for NS glasses, and (c) for KS glasses.

is evident, as seen in Fig. 5. For v-SiO_2, it has been demonstrated by Y. Inamura *et al.*[83] that the transformation of the Q_4 units to Q_6 units leads to a suppression of the BP modes that is manifested by a decrease in the BP intensity. The study has also shown that the number of modes in the BP is almost proportional to the volume which is in agreement with our findings.

A possible origin of such a correlation has been suggested through the study of Yang *et al.*[84] in metallic glasses. According to this study, the origin of the vibrations that create the vibrational excess of low frequencies in amorphous solids is related to the structure of the Voronoi polyhedron around each atom. These polyhedra, which characterize the closest points of the central atom to its neighbors, are distributed in different directions at varying distances. This unfound diversity in crystals, usually created by disorder in glasses, adds some degrees of freedom to the central atom where vibrations can occur. In the case of the vibrations of the BP, it has been shown that the displacement of atoms in the direction of the furthest corner of the polyhedron corresponds to the BP. The study extended to several types of metallic glasses and could explain the topological origin of BP from the local structure of atoms.

On the other hand, previous reports on inelastic neutron scattering and hyper-Raman spectroscopy[44,85,86] have argued that the modes giving rise to the BP are produced by rotational motions of several interconnected tetrahedral SiO_4 units in vitreous silica. The Q_4 units being the building units of vitreous silica, we investigate next, based on the ideas brought by these experiments, the relationship of the BP with Q_4 unit vibrations. We have calculated the vibrational mean square displacement (MSD) of these units in all studied systems and compared them with the BP intensity as shown in Fig. 8 and 9. More details about the calculated MSDs can be found in the ESI†[36] where the MSDs were calculated for each system in different compositions at 50 K, the same temperature at which the VDOS was evaluated.

Fig. 8 displays the BP intensity as a function of the vibrational MSD of the Q_4 units for BTS and CAS. Two tendencies are observed for the CAS glasses: (i) with increasing the amount of Al_2O_3 from 5% to 15%, the BP intensity decrease is accompanied by an increase in the vibrational MSD of the Q_4 units, and (ii) for concentrations between 20% and 30%, the decrease of the BP intensity is followed by a decrease in the vibrational MSD of the Q_4 units in the system. Unlike the BTS system, the nonlinear trend observed for the CAS is mainly coming from the chosen stoichiometry of the CAS glasses in which Al_2O_3 is varied as a function of CaO–SiO_2. As discussed by Atila *et al.*,[31] the role of Ca can be relative in different regions of composition. From 5% to 15% the BP intensity decrease appears to be

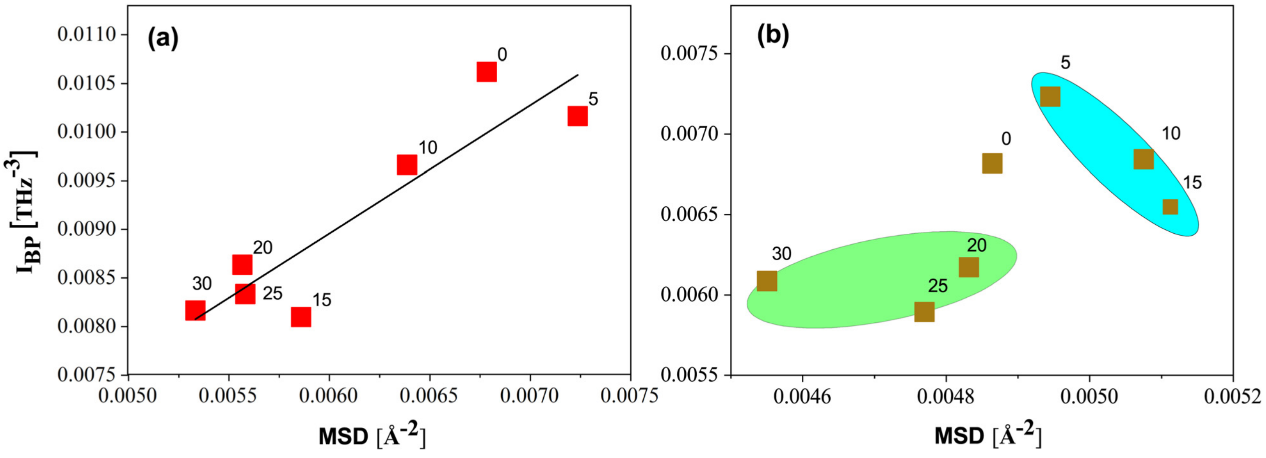

Fig. 8 The intensity of the BPs of VDOS as a function of the vibrational mean square displacement of Q_4 units for silicate with intermediate oxides. (a) For the BTS and (b) for the CAS glasses. The numbers are the concentrations in (%) and the line and circles are guides for the eyes.

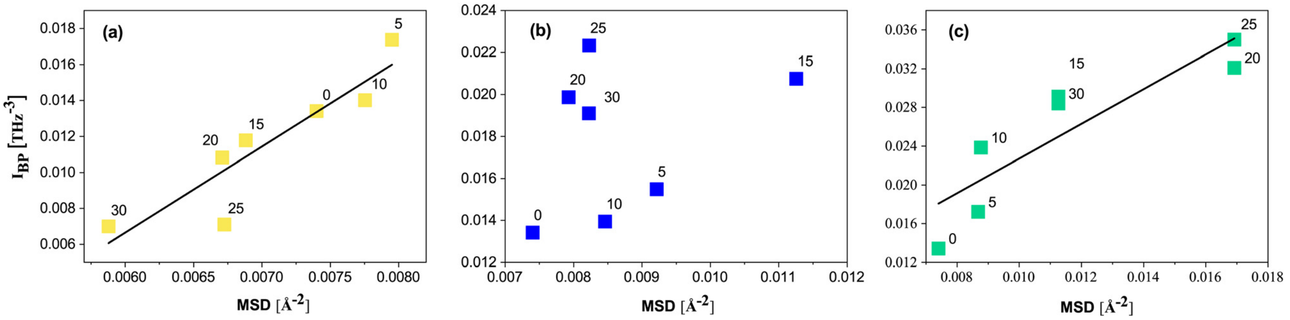

Fig. 9 The intensity of the BPs of VDOS as a function of the vibrational mean square displacement of Q_4 units for silicate with alkali oxide modifiers. (a) For LS glasses, (b) for NS glasses, and (c) for KS glasses. The numbers are the concentrations in (%) and the lines are a guide for the eyes.

more related to the decrease of Ca content. This is manifested by the increase in the vibrational MSD of the Q_4 units, which is the signature of the modifier role of Ca cations that gives more degrees of freedom to the Q_4 units in the system. For compositions above 15%, the role of Al as a network former start to influence in a similar manner to TiO_2 in BTS glasses the BP intensity and follows a linear decrease as Al_2O_3 content increases. The decrease observed in the vibrational MSD of Q_4 units is attributed to two factors; the first one is related to the role of Ca cations that changes from network modifier to charge compensator, which results in the decrease of the degrees of freedom of the Q_4 units in the overall network. The second is a consequence of the increase of Al_2O_3 which results in the increased network connectivity and reduces the mobility of these Q_4 units.[31] This intriguing observation reported on the CAS system shows that the Q_4 unit vibration does affect systematically the BP intensity upon increasing the intermediate content, even if the content of the modifier is affecting the MSD of Q_4 units.

For the BTS, Fig. 8 represents the I_{BP} as a function of the vibrational MSD of the Q_4 units. A positive correlation is found when the BP intensity decreases along with the decrease in the vibrational MSD of the Q_4 units. This decrease attributed to the act of TiO_2 is a consequence of the creation of more Q_4 units and more BOs[30] that increase the stiffness of the glass. This has been previously linked to several parameters such as network connectivity,[87] pressure[88] and density,[89] with similar effect on the BP intensity with the variation of the amount of the intermediate cation in the system. It is also important to mention that when replacing Si with Ti, the network requires the presence of a charge compensating cation, which inhibits liberation of TiO_4 tetrahedra and thus yields a lower BP intensity. In addition to that, the substitution of Si with Ti, which has a medium size comparable to Si, reduces the vibrations of the Q_4 units and therefore reduces their contribution to the BP intensity.

In the case of network-modifying cations, Fig. 9(b) displays the BP intensity as a function of the vibrational MSD of the Q_4 units in alkali silicate glasses. The increase of lithium amount in LS glasses leads to a decrease of the Q_4 units vibrational MSD and a decrease in the BP intensity. For the KS glasses, a positive correlation between the I_{BP} and MSD of the Q_4 units was observed, but not as clear as the one reported for intermediate oxides. Because of that, one may assume that the vibrations of those units are not the only vibrations that contribute to the BP excitations. This is because the addition of K cations depolymerizes the network and therefore creates more structural Q_3 and Q_2 units along with a decrease in the number of Q_4 units. Based on that, we have decided to calculate the vibrational MSD of other units considering their fractions. The fractional MSD of the Q_n units was calculated using this equation:

$$f^{i}_{\mathrm{MSD}} = \frac{Q_{\mathrm{i}}}{Q_{\mathrm{t}}}\langle \mathrm{MSD}(Q_{\mathrm{i}})\rangle, \quad i = 2, 3, 4 \tag{5}$$

where Q_i and Q_t are the partial and the total number of Q_n units, respectively. Fig. 10 shows intensities of the BP as a function of the fractional vibrational MSD of Q_n units in KS glasses. A positive correlation was found for KS glasses where the BP intensity increases with the increase of the vibrational MSD of Q_3 and Q_2 units. This indicates that the increase observed in the intensity of the BP is attributed to the increase in the vibrational MSDs of all these units. For the NS glasses, no clear correlation was found between these units. To discuss these results, one should take into consideration different factors. The first is the fact that the BP in binary silicate glasses depends on the liberation of the interconnected Q_4 units as observed for the KS glasses. This is demonstrated in Section 2, where the vibrations of K cations appeared to be in the vibrational spectrum for frequencies below 11 THz. So, one may assume that there is a contribution of these element vibrations in the BP excitations. This observation based on the work of Richet and Mcintosh *et al.*[21,23] indicates that the BP is related to the localized vibrations of the network modifier cations. On the other hand, the increase of the concentration of the alkali oxide modifiers results in increasing the number of NBOs which consequently increase the contribution of these vibrations to the BP as suggested by Mcintosh *et al.* and Richet.[23,90] Since, cations of the same size could affect the BP differently as demonstrated by Griebenow *et al.*,[91] the ionic field strength of the cation, also play an important role in this matter. As we found for Li, which gives a similar behavior to network intermediate oxides because of its strong bending, it tightens the network in contrast to K cations as asserted.

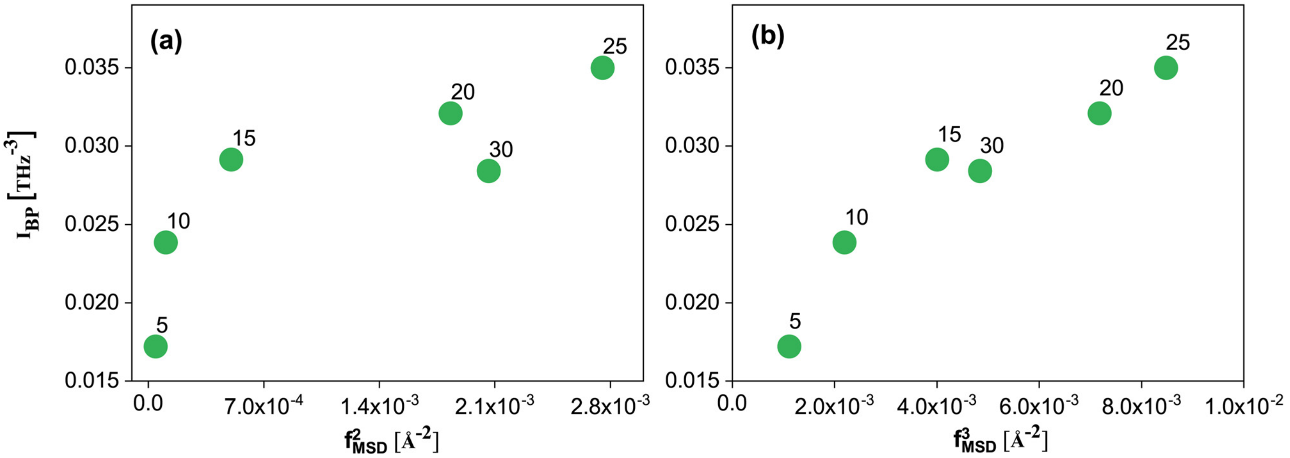

Fig. 10 The intensity of the BPs of VDOS as a function of the vibrational MSD of Q_n units for the KS glass. (a) For the Q_2 units and (b) for the Q_3 units. The numbers are the concentration of potassium in %.

4. Conclusions

In this paper, the effect of different types of oxides on the vibrational spectrum of silica glasses was studied. The effect of alkali oxides on different vibration modes has been shown to differ between Li and other alkalis, especially at the intermediate frequencies. Likewise, for the effect on the BP, the addition of alkaline oxides showed a clear dependence on the nature of the alkalis, thus questioning the classification of Li_2O as a modifier oxide. As for the effect of the intermediate oxides studied, homogeneity in the behavior of the vibrational spectrum and the BP was found. A captivating similarity between the compositional tendency of the intermediate oxides and that of Li_2O has been reported, thus suggesting a pseudo-intermediate character of Li cations in LS glasses. In addition to the empirical correlation reproduced by our simulations between the intensity of the BP and the C_{44} shear modulus, a new correlation was first suggested between the BP and the Voronoi atomic volumes of Q_4 and Q_3 units together with their vibrational MSDs. Indeed, further study is needed to examine why VAV governs the nature of the BP arising from excess VDOS, not to mention the apparent deviation of the Q_3 VAV and vibrational MSDs for high concentrations (30% especially, Fig. 7 and 8 in KS glasses) which indicates a significant change in the glass structure. Because binary silicate glasses with high alkali modifier concentrations are difficult to produce experimentally, MD simulations may be an efficient way to examine this behavior in the future. Nonetheless, we believe that the insights provided in this paper, the origin of BP in the studied silicate glasses with different compositions, including binary and ternary glasses, will provide significant insight into the physics of the vitreous state, opening a gate toward the physical modes responsible for these established correlations.

Conflicts of interest

There are no conflicts to declare.

Notes and references

1 R. Zeller and R. Pohl, *Phys. Rev. B: Solid State*, 1971, **4**, 2029.
2 W. A. Phillips and A. Anderson, *Amorphous solids: low-temperature properties*, Springer, 1981, vol. 24.
3 K. Binder and W. Kob, *Glassy materials and disordered solids: An introduction to their statistical mechanics*, World scientific, 2011.
4 T. Ohsaka and S. Oshikawa, *Phys. Rev. B: Condens. Matter Mater. Phys.*, 1998, **57**, 4995.
5 T. Ohsaka and T. Ihara, *Phys. Rev. B: Condens. Matter Mater. Phys.*, 1994, **50**, 9569.
6 G. Johari, *J. Non-Cryst. Solids*, 2002, **307**, 114–127.
7 M. F. Ando, O. Benzine, Z. Pan, J.-L. Garden, K. Wondraczek, S. Grimm, K. Schuster and L. Wondraczek, *Sci. Rep.*, 2018, **8**, 1–14.
8 T. Nakayama, *Rep. Prog. Phys.*, 2002, **65**, 1195.
9 S. Kojima, Y. Matsuda, Y. Fukawa, M. Kawashima, Y. Moriya, T. Yamada, O. Yamamuro and M. Kodama, *J. Non-Cryst. Solids*, 2010, **356**, 2524–2527.
10 M. Kofu, Y. Inamura, Y. Moriya, A. Podlesnyak, G. Ehlers and O. Yamamuro, *J. Mol. Liq.*, 2015, **210**, 164–168.
11 T. S. Grigera, V. Martn-Mayor, G. Parisi and P. Verrocchio, *Nature*, 2003, **422**, 289–292.
12 V. Karpov, I. Klinger and F. Ignat'Ev, *Zh. Eksp. Teor. Fiz.*, 1983, **84**, 775.
13 L. Gil, M. Ramos, A. Bringer and U. Buchenau, *Phys. Rev. Lett.*, 1993, **70**, 182.
14 L. Gartner and E. Lerner, *SciPost Phys.*, 2016, **1**, 016.
15 E. Duval and A. Mermet, *Phys. Rev. B: Condens. Matter Mater. Phys.*, 1998, **58**, 8159.
16 A. Marruzzo, W. Schirmacher, A. Fratalocchi and G. Ruocco, *Sci. Rep.*, 2013, **3**, 1–7.
17 W. Schirmacher, G. Ruocco and T. Scopigno, *Phys. Rev. Lett.*, 2007, **98**, 025501.
18 T. C. Hufnagel, *Nat. Mater.*, 2015, **14**, 867–868.

19 H. R. Schober, U. Buchenau and V. Gurevich, *Phys. Rev. B: Condens. Matter Mater. Phys.*, 2014, **89**, 014204.

20 Y.-C. Hu and H. Tanaka, *Nat. Phys.*, 2022, **18**, 669–677.

21 N. F. Richet, *J. Chem. Phys.*, 2012, **136**, 034703.

22 B. Hehlen and D. R. Neuville, *Phys. Chem. Chem. Phys.*, 2020, **22**, 12724–12731.

23 C. McIntosh, J. Toulouse and P. Tick, *J. Non-Cryst. Solids*, 1997, **222**, 335–341.

24 N. F. Richet, *Phys. B*, 2009, **404**, 3799–3806.

25 N. Shimodaira, K. Saito, N. Hiramitsu, S. Matsushita and A. Ikushima, *Phys. Rev. B: Condens. Matter Mater. Phys.*, 2005, **71**, 024209.

26 A. Hassan, L. Börjesson and L. Torell, *J. Non-Cryst. Solids*, 1994, **172**, 154–160.

27 K. Nakamura, Y. Takahashi, M. Osada and T. Fujiwara, *J. Ceram. Soc. Jpn.*, 2013, **121**, 1012–1014.

28 V. Novikov and A. Sokolov, *Solid State Commun.*, 1991, **77**, 243–247.

29 S. Elliott, *Phys. Rev. Lett.*, 1991, **67**, 711.

30 E. M. Ghardi, A. Atila, M. Badawi, A. Hasnaoui and S. Ouaskit, *J. Am. Ceram. Soc.*, 2019, **102**, 6626–6639.

31 A. Atila, E. M. Ghardi, A. Hasnaoui and S. Ouaskit, *J. Non-Cryst. Solids*, 2019, **525**, 119470.

32 E. M. Ghardi, H. Jabraoui, M. Badawi, A. Hasnaoui, S. Ouaskit and Y. Vaills, *J. Phys. Chem. B*, 2020, **124**, 9216–9223.

33 A. Pedone, G. Malavasi, M. C. Menziani, A. N. Cormack and U. Segre, *J. Phys. Chem. B*, 2006, **110**, 11780–11795.

34 M. Bouhadja, N. Jakse and A. Pasturel, *J. Chem. Phys.*, 2014, **140**, 234507.

35 S. Sundararaman, L. Huang, S. Ispas and W. Kob, *J. Chem. Phys.*, 2019, **150**, 154505.

36 Supplementary Materials, URL_will_be_inserted_by_publisher.

37 A. P. Thompson, H. M. Aktulga, R. Berger, D. S. Bolintineanu, W. M. Brown, P. S. Crozier, P. J. Int Veld, A. Kohlmeyer, S. G. Moore, T. D. Nguyen, R. Shan, M. J. Stevens, J. Tranchida, C. Trott and S. J. Plimpton, *Comput. Phys. Commun.*, 2022, **271**, 108171.

38 P. Desmarchelier, K. Termentzidis and A. Tanguy, *Semicond. Sci. Technol.*, 2020, **35**, 094001.

39 A. Pedone, G. Malavasi, A. N. Cormack, U. Segre and M. C. Menziani, *Chem. Mater.*, 2007, **19**, 3144–3154.

40 J. F. Nye *et al.*, *Physical properties of crystals: their representation by tensors and matrices*, Oxford University Press, 1985.

41 N. Zotov, *J. Non-Cryst. Solids*, 2001, **287**, 231–236.

42 J. Luo, N. J. Smith, C. G. Pantano and S. H. Kim, *J. Non-Cryst. Solids*, 2018, **494**, 94–103.

43 J. Sarnthein, A. Pasquarello and R. Car, *Science*, 1997, **275**, 1925–1927.

44 U. Buchenau, M. Prager, N. Nücker, A. Dianoux, N. Ahmad and W. Phillips, *Phys. Rev. B: Condens. Matter Mater. Phys.*, 1986, **34**, 5665.

45 B. Guillot and Y. Guissani, *Phys. Rev. Lett.*, 1997, **78**, 2401.

46 E. Courtens, M. Foret, B. Hehlen and R. Vacher, *Solid State Commun.*, 2001, **117**, 187–200.

47 V. Mazzacurati, G. Ruocco and M. Sampoli, *EPL*, 1996, **34**, 681.

48 N. Zotov, I. Ebbsjö, D. Timpel and H. Keppler, *Phys. Rev. B: Condens. Matter Mater. Phys.*, 1999, **60**, 6383.

49 Z. Zhang, S. Ispas and W. Kob, *J. Chem. Phys.*, 2020, **153**, 124503.

50 D. Kilymis, S. Ispas, B. Hehlen, S. Peuget and J.-M. Delaye, *Phys. Rev. B*, 2019, **99**, 054209.

51 M. Wilson, P. A. Madden, M. Hemmati and C. A. Angell, *Phys. Rev. Lett.*, 1996, **77**, 4023.

52 S. Taraskin and S. Elliott, *Phys. Rev. B: Condens. Matter Mater. Phys.*, 1997, **56**, 8605.

53 J. Zhao, P. Gaskell, L. Cormier and S. Bennington, *Phys. B*, 1997, **241**, 906–908.

54 P. Ganster, M. Benoit, W. Kob and J.-M. Delaye, *J. Chem. Phys.*, 2004, **120**, 10172–10181.

55 S. Ispas, N. Zotov, S. De Wispelaere and W. Kob, *J. Non-Cryst. Solids*, 2005, **351**, 1144–1150.

56 L.-G. Hwa, S.-L. Hwang and L.-C. Liu, *J. Non-Cryst. Solids*, 1998, **238**, 193–197.

57 B. Hehlen and D. Neuville, *J. Phys. Chem. B*, 2015, **119**, 4093–4098.

58 J. Qi, Q. Liu, M. Cao, Y. Zhao, H. Hao, Z. Yao and H. Liu, *J. Eur. Ceram. Soc.*, 2020, **40**, 3027–3034.

59 P. Van Aken, T. Höche, F. Heyroth, R. Keding and R. Uecker, *Phys. Chem. Miner.*, 2004, **31**, 543–552.

60 S. Markgraf, S. Sharma and A. Bhalla, *J. Mater. Res.*, 1993, **8**, 635–648.

61 G. S. Henderson and M. E. Fleet, *Can. Mineral.*, 1995, **33**, 399–408.

62 S. Stassen, P. Tarte and A. Rulmont, *Spectrochim. Acta, Part A*, 1998, **54**, 1423–1431.

63 K. Nakamura, Y. Takahashi and T. Fujiwara, *Sci. Rep.*, 2014, **4**, 1–4.

64 G. Blasse, *J. Inorg. Nucl. Chem.*, 1979, **41**, 639–641.

65 A. Sokolov, A. Kisliuk, M. Soltwisch and D. Quitmann, *Phys. Rev. Lett.*, 1992, **69**, 1540.

66 E. Duval, A. Boukenter and T. Achibat, *J. Phys.: Condens. Matter*, 1990, **2**, 10227.

67 F. Leonforte, R. Boissiere, A. Tanguy, J. Wittmer and J.-L. Barrat, *Phys. Rev. B: Condens. Matter Mater. Phys.*, 2005, **72**, 224206.

68 F. Leonforte, A. Tanguy, J. Wittmer and J.-L. Barrat, *Phys. Rev. Lett.*, 2006, **97**, 055501.

69 J. Schroeder, W. Wu, J. L. Apkarian, M. Lee, L.-G. Hwa and C. T. Moynihan, *J. Non-Cryst. Solids*, 2004, **349**, 88–97.

70 G. Carini Jr, G. Carini, D. Cosio, G. D'Angelo and F. Rossi, *Philos. Mag.*, 2016, **96**, 761–773.

71 O. Benzine, Z. Pan, C. Calahoo, M. Bockowski, M. M. Smedskjaer, W. Schirmacher and L. Wondraczek, *Sci. Rep.*, 2021, **11**, 1–12.

72 Z. Pan, O. Benzine, S. Sawamura, R. Limbach, A. Koike, T. D. Bennett, G. Wilde, W. Schirmacher and L. Wondraczek, *Phys. Rev. B*, 2021, **104**, 134106.

73 H. Shintani and H. Tanaka, *Nat. Mater.*, 2008, **7**, 870–877.

74 A. Atila, Y. Ouldhnini, S. Ouaskit and A. Hasnaoui, *Phys. Rev. B*, 2022, **105**, 134101.

75 A. Atila, E. M. Ghardi, S. Ouaskit and A. Hasnaoui, *Phys. Rev. B*, 2019, **100**, 144109.

76 W. H. Zachariasen, *J. Am. Chem. Soc.*, 1932, **54**, 3841–3851.

77 A. Dietzel, *Z. Elektrochem. Angew. Phys. Chem.*, 1942, **48**, 9–23.

78 K.-H. Sun, *J. Am. Ceram. Soc.*, 1947, **30**, 277–281.

79 A. K. Varshneya, *Fundamentals of inorganic glasses*, Elsevier, 2013.

80 N. P. Bansal and R. H. Doremus, *Handbook of glass properties*, Elsevier, 2013.

81 J. Du and L. R. Corrales, *J. Non-Cryst. Solids*, 2006, **352**, 3255–3269.

82 C. Calahoo and L. Wondraczek, *J. Non-Cryst. Solids: X*, 2020, **8**, 100054.

83 Y. Inamura, M. Arai, M. Nakamura, T. Otomo, N. Kitamura, S. Bennington, A. Hannon and U. Buchenau, *J. Non-Cryst. Solids*, 2001, **293**, 389–393.

84 J. Yang, Y.-J. Wang, E. Ma, A. Zaccone, L. Dai and M. Jiang, *Phys. Rev. Lett.*, 2019, **122**, 015501.

85 U. Buchenau, N. Nücker and A. Dianoux, *Phys. Rev. Lett.*, 1984, **53**, 2316.

86 B. Hehlen, E. Courtens, A. Yamanaka and K. Inoue, *J. Non-Cryst. Solids*, 2002, **307**, 87–91.

87 P. Chen, C. Holbrook, P. Boolchand, D. Georgiev, K. Jackson and M. Micoulaut, *Phys. Rev. B: Condens. Matter Mater. Phys.*, 2008, **78**, 224208.

88 B. Mantisi, S. Adichtchev, S. Sirotkin, L. Rafaelly, L. Wondraczek, H. Behrens, C. Marcenat, N. Surovtsev, A. Pillonnet and E. Duval, *et al.*, *J. Phys.: Condens. Matter*, 2009, **22**, 025402.

89 Y. Inamura, M. Arai, T. Otomo, N. Kitamura and U. Buchenau, *Phys. B*, 2000, **284**, 1157–1158.

90 N. F. Richet, H. Kawaji and T. Rouxel, *J. Chem. Phys.*, 2010, **133**, 044510.

91 K. Griebenow, C. B. Bragatto, E. I. Kamitsos and L. Wondraczek, *J. Non-Cryst. Solids*, 2018, **481**, 447–456.